

## Modulating Two-Dimensional Non-Close-Packed Colloidal Crystal Arrays by Deformable Soft Lithography

Xiao Li, Tieqiang Wang, Junhu Zhang,\* Xin Yan, Xuemin Zhang, Difu Zhu, Wei Li, Xun Zhang, and Bai Yang

State Key Laboratory of Supramolecular Structure and Materials, College of Chemistry, Jilin University, Changchun 130012, P. R. China

Received July 23, 2009. Revised Manuscript Received August 13, 2009

We report a simple method to fabricate two-dimensional (2D) periodic non-close-packed (ncp) arrays of colloidal microspheres with controllable lattice spacing, lattice structure, and pattern arrangement. This method combines soft lithography technique with controlled deformation of polydimethylsiloxane (PDMS) elastomer to convert 2D hexagonal close-packed (hcp) silica microsphere arrays into ncp ones. Self-assembled 2D hcp microsphere arrays were transferred onto the surface of PDMS stamps using the lift-up technique, and then their lattice spacing and lattice structure could be adjusted by solvent swelling or mechanical stretching of the PDMS stamps. Followed by a modified microcontact printing ( $\mu$ cp) technique, the as-prepared 2D ncp microsphere arrays were transferred onto a flat substrate coated with a thin film of poly(vinyl alcohol) (PVA). After removing the PVA film by calcination, the ncp arrays that fell on the substrate without being disturbed could be lifted up, deformed, and transferred again by another PDMS stamp; therefore, the lattice feature could be changed step by step. Combining isotropic solvent swelling and anisotropic mechanical stretching, it is possible to change hcp colloidal arrays into full dimensional ncp ones in all five 2D Bravais lattices. This deformable soft lithography-based lift-up process can also generate patterned ncp arrays of colloidal crystals, including one-dimensional (1D) microsphere arrays with designed structures. This method affords opportunities and spaces for fabrication of novel and complex structures of 1D and 2D ncp colloidal crystal arrays, and these as-prepared structures can be used as molds for colloidal lithography or prototype models for optical materials.

### Introduction

Colloidal crystals made of polymer or inorganic microspheres have attracted extensive interest due to their potential applications as sensing,<sup>1</sup> optical,<sup>2,3</sup> and photonic bandgap materials<sup>4</sup> as well as templates for fabrication of highly ordered macroporous materials<sup>5</sup> and biopatterns.<sup>6</sup> Generally, two-dimensional (2D) colloidal crystal arrays are more attractive for their considerable fundamental and technological importance in nanosphere lithography,<sup>7</sup> optical devices,<sup>8</sup> and model systems for 2D crystallization.<sup>9</sup> Therefore, various manipulation techniques based on electrostatic,<sup>10</sup> optical tweezers,<sup>11</sup> dip-pen nanolithography,<sup>12</sup> or AFM<sup>13</sup> have been developed to prepare 2D colloidal microsphere arrays with designed structures for their ability to place each microsphere at a desired position. Although these approaches are not limited by structure complexity, they suffered from being expensive, time-consuming, and difficult to apply in large area

constructions. As an alternative strategy, self-assembly techniques based on gravity sedimentation,<sup>14</sup> electrostatic interactions,<sup>15,16</sup> and capillary force<sup>17</sup> have been developed in the past decades, which are capable of producing large, single-crystalline domains; however, they are limited to fabricate colloidal crystal films with hexagonal close-packed (hcp) arrays due to the thermodynamically lowest state.

In comparison with close-packed colloidal crystals, non-close-packed (ncp) ones possess a wider photonic band gap,<sup>18</sup> which makes them important for applications in photonic materials, including light-emitting diodes,<sup>19</sup> all-optical chips,<sup>20</sup> and optical switches.<sup>21</sup> In addition, ncp arrays are also pursued for applications in expanding the complexity of inverse opals fabrication due to their high void-filling fraction<sup>18</sup> as well as in making tunable superhydrophobic surface,<sup>22</sup> etc. Benefiting from the above reasons, various techniques, such as template-induced growth technique,<sup>23–25</sup> colloidal epitaxy method,<sup>26</sup> electrostatic

\*Corresponding author. E-mail: zjh@jlu.edu.cn.

(1) Weissman, J. M.; Sunkara, H. B.; Tse, A. S.; Asher, S. A. *Science* **1996**, *274*, 959.

(2) Xia, Y.; Gates, B.; Yin, Y.; Lu, Y. *Adv. Mater.* **2000**, *12*, 693.

(3) Kim, S. H.; Jeon, S. J.; Yang, S. M. *J. Am. Chem. Soc.* **2008**, *130*, 6040.

(4) John, S. *Phys. Rev. Lett.* **1987**, *58*, 2486.

(5) Holland, B. T.; Blanford, C. F.; Stein, A. *Science* **1998**, *281*, 538.

(6) Yap, F. L.; Zhang, Y. *Biosens. Bioelectron.* **2007**, *22*, 775.

(7) Kosiorok, A.; Kandulski, W.; Chudzinski, P.; Kempa, K.; Giersig, M. *Nano Lett.* **2004**, *4*, 1359.

(8) Zhao, Y.; Avrutsky, I. *Opt. Lett.* **1999**, *24*, 817.

(9) Eisenmann, C.; Gasser, U.; Keim, P.; Maret, G. *Phys. Rev. Lett.* **2004**, *93*, 105702.

(10) Pertsinidis, A.; Ling, X. S. *Phys. Rev. Lett.* **2001**, *87*, 098303.

(11) Hoogenboom, J. P.; Vossen, D. L. J.; Faivre-Moskalenko, C.; Dogterom, M.; Van Blaaderen, A. *Appl. Phys. Lett.* **2002**, *80*, 4828.

(12) Demers, L. M.; Mirkin, C. A. *Angew. Chem., Int. Ed.* **2001**, *40*, 3069.

(13) Junno, T.; Deppert, K.; Montelius, L.; Samuelson, L. *Appl. Phys. Lett.* **1995**, *66*, 3627.

(14) Donselaar, L. N.; Philipse, A. P.; Suurmond, J. *Langmuir* **1997**, *13*, 6018.

(15) Larsen, A. E.; Grier, D. G. *Nature* **1997**, *385*, 230.

(16) Ma, L. C.; Subramanian, R.; Huang, H. W. *Nano Lett.* **2007**, *7*, 439.

(17) Dushkin, C. D.; Nagayama, K.; Miwa, T.; Kralchevsky, P. A. *Langmuir* **1993**, *9*, 3695.

(18) Doosje, M.; Hoenders, B. J.; Knoester, J. *J. Opt. Soc. Am. B* **2000**, *17*, 600.

(19) Yablonovitch, E. *J. Opt. Soc. Am. B* **1993**, *10*, 283.

(20) Lin, S. Y.; Chow, E.; Hietala, V.; Villeneuve, P. R.; Joannopoulos, J. D. *Science* **1998**, *282*, 274.

(21) Weissman, J. M.; Sunkara, H. B.; Tse, A. S.; Asher, S. A. *Science* **1996**, *274*, 959.

(22) Han, J. T.; Lee, D. H.; Ryu, C. Y.; Cho, K. *J. Am. Chem. Soc.* **2004**, *126*, 4796.

(23) Koh, S. J. *Nanoscale Res. Lett.* **2007**, *2*, 519.

(24) Xia, Y. N.; Yin, Y. D.; Lu, Y. *Adv. Funct. Mater.* **2003**, *13*, 907.

(25) Lu, Y.; Yin, Y. D.; Xia, Y. N. *Adv. Mater.* **2001**, *13*, 34.

(26) Velikov, K. P.; Christova, C. G.; Dullens, R. P. A.; van Blaaderen, A. *Science* **2002**, *296*, 106.

funneling technique,<sup>27</sup> and colloidal configurations in aqueous suspensions,<sup>28</sup> have been developed. Fenolosa and Meseguer<sup>29</sup> combined thermal sintering and etching techniques to fabricate ncp silica microspheres connected with silica cylinders. Haginoya et al.<sup>30</sup> and Tan et al.<sup>31</sup> made use of reactive ion etching to modify a self-assembled 2D array of polystyrene microspheres into periodic nanoscale-rugged structures. However, these fabrication processes sacrifice particle size, and the largest spacing depends on the diameter of microsphere. Jiang et al.<sup>32</sup> developed a robust spin-coating technique for assembling ncp colloidal microsphere arrays. They further extended the work to develop a generalized templating approach for fabricating wafer-scale ncp colloidal crystals from a variety of functional materials, without developing synthetic methods for highly uniform colloids of each material.<sup>33</sup> These techniques could be used to obtain ncp arrays with specific lattice spacing, but the lattice spacing is not controllable. Moreover, many methods of fabricating ncp colloidal crystal encounter difficulties in modulating new lattice structures rather than hexagonal, which is the entropy favorable state of 2D self-assembled colloidal microspheres.

As is well-known, there are five distinct Bravais lattices in two dimensions. Classified by two basis vectors and the angle between them, these five lattices are hexagonal, oblique, rectangular, square, and centered rectangular, which have different lattice symmetry and spatial parameters. The lattice structure and lattice spacing act on manipulating the photonic bandgaps of photonic crystal, which play a significant role in the realization of integrated optical circuit devices.<sup>34</sup> Therefore, it is of great importance to find a facile, high-efficiency, and low-cost method to fabricate 2D colloidal microsphere arrays in all five 2D Bravais lattice.

Recently, our research group has developed a lift-up and transfer-printing method to fabricate 2D ncp colloidal microsphere arrays.<sup>35</sup> PDMS elastomer stamps were used to lift up 2D self-assembled close-packed colloidal crystal arrays and were then deformed by solvent swelling or mechanical stretching to adjust the lattice structures of 2D arrays of microspheres. Using this method, we can tune the interparticle distance or change the lattice structure of the 2D ncp colloidal crystals. In this paper, we report further developments of this soft lithography-based technique. By repeating lift-up and transfer printing, now we can adjust the lattice spacing and lattice structure of the ncp colloidal microsphere arrays more freely. Accordingly, we can produce colloidal microsphere arrays in all 2D primitive Bravais lattices. Furthermore, by introducing morphology-patterned PDMS elastomer sheet into this system, patterned ncp arrays of colloidal crystals were also achieved. The novel structures obtained could be used not only as molds for colloidal lithography but also as models for optical materials.

## Experimental Section

**Materials.** Monodispersed silica microspheres ( $560 \pm 15$  nm) were prepared in ethanol according to the Stöber method.<sup>36</sup>

(27) Huang, H. W.; Bhadrachalam, P.; Ray, V. *Appl. Phys. Lett.* **2008**, *93*, 073110.

(28) Yethiraj, A.; van Blaaderen, A. *Nature* **2003**, *421*, 513.

(29) Fenolosa, R.; Meseguer, F. *Adv. Mater.* **2003**, *15*, 1282.

(30) Haginoya, C.; Ishibashi, M.; Koike, K. *Appl. Phys. Lett.* **1997**, *71*, 2934.

(31) Tan, B. J.-Y. *J. Phys. Chem. B* **2004**, *108*, 18575.

(32) Jiang, P. *Appl. Phys. Lett.* **2006**, *89*, 011908.

(33) Venkatesh, S.; Jiang, P.; Jiang, B. *Langmuir* **2007**, *23*, 8231.

(34) Joannopoulos, J. D.; Mead, R. D.; Winn, J. N. *Photonic Crystal: Molding the Flow of Light*; Princeton University Press: Princeton, NJ, 1995.

(35) Yan, X.; Yao, J. M.; Lu, G.; Li, X.; Zhang, J. H.; Han, K.; Yang, B. *J. Am. Chem. Soc.* **2005**, *127*, 7688.

(36) Stöber, W.; Fink, A.; Bohn, E. *J. Colloid Interface Sci.* **1968**, *26*, 62.

Silicon (100) wafers were cleaned by immersion into a solution of concentrated  $\text{H}_2\text{SO}_4:\text{H}_2\text{O}_2$  (v/v: 7/3) for about 5 h at 90 °C and then rinsed with a large amount of distilled water and dried by nitrogen gas. Polydimethylsiloxane (PDMS) elastomer kits (Sylgard 184) were purchased from Dow Corning (Midland, MI). Sulfuric acid, hydrogen peroxide, poly(vinyl alcohol) (PVA), and ethanol were used as received.

Ncp colloidal microsphere arrays. 2D colloidal crystals were formed by the evaporation of suspension, which was based on the method described by Micheletto and collaborators.<sup>37</sup> In a typical lift-up process, a PDMS stamp was wetted by ethanol and then applied to the 2D colloidal crystal film. After the evaporation of the ethanol, the sample was heated at 100 °C for 3 h. The PDMS stamp was carefully peeled away, and a single layer of 2D colloidal crystals was transferred onto the surface of PDMS by using the lift-up soft lithography we reported.<sup>38</sup> The PDMS stamp containing the silica microspheres was swollen with toluene solution (process I) or stretched along one direction (process II). It was worth noting that the two sides of PDMS orthogonal to the stretching direction were fastened by clamps with little touching points. The device and detailed operation were in the Supporting Information of ref 35. The deformed PDMS stamp was brought into contact with the PVA-coated substrate under a pressure of about  $0.2 \times 10^5$  Pa. After that, the system was heated at 100 °C for 1.5 h. After peeling away the PDMS stamp carefully, 2D ncp silicon microsphere arrays were achieved on the PVA-surface. After sintering at 400 °C for 2 h, the PVA film disappeared and the silicon microspheres fell on the substrate. By employing a second lift-up soft lithography, the ncp microspheres were transferred to the surface of PDMS film, which was subsequently referred to here as the second-generation stamp and swollen with toluene or stretched in the next cycle. The obtained 2D ncp microsphere arrays with further changed arrangement on the deformed PDMS film were transferred to the substrate coated with a film of PVA. By employing the cyclical process—(1) lift-up; (2) enlarge lattice space by swelling or stretching; (3) transfer to the PVA surface; (4) remove PVA film by sintering appropriate times—2D ncp microsphere arrays of all five Bravais lattices could be fabricated.

Patterned ncp colloidal microsphere arrays. PDMS stamp with strips or posts patterned features was applied to the 2D ncp colloidal crystal film we have obtained above. After the evaporation of the ethanol, the sample was heated at 100 °C for 3 h. Then the ncp colloidal crystal was transferred onto the surface of PDMS, which could be kept on the PVA-coated substrate subsequently. In addition, in the lift-up process, patterned PDMS stamp can be deformed under capillary force and mechanical stress during the transfer process. Here, the relief features on the PDMS stamp were ordered square arrays of posts with diameter of 6.6  $\mu\text{m}$  and height of 1.4  $\mu\text{m}$ , and they were separated by  $\sim 7.6 \mu\text{m}$  or ordered arrays of strips with 9  $\mu\text{m}$  wide and separated by 11  $\mu\text{m}$ . The mixing ratio between the polymer precursor and the curing agent were tuned to 10:0.90 and 10:1.0, corresponding to soft and hard PDMS stamp, respectively. At the deformation equilibrium state of PDMS stamp, small voids were formed around the edges of the protruding regions of the stamp. After the lift-up operation, microspheres in these areas remain and generate patterned one-dimensional ncp arrays.

**Characterization.** Scanning electron microscopy (SEM) images were taken with a JEOL FESEM 6700F electron microscope with primary electron energy of 3 kV, and samples were sputtered with a layer of Pt (ca. 2 nm thick) prior to imaging to improve conductivity.

## Results and Discussion

**1. Lift-up and Microcontact Printing of 2D Colloidal Crystals.** Figure 1 shows the schematic procedures of the

(37) Micheletto, R.; Fukuda, H.; Ohtsu, M. *Langmuir* **1995**, *11*, 3333.

(38) Yao, J.; Yan, X.; Lu, G.; Zhang, K.; Chen, X.; Jiang, L.; Yang, B. *Adv. Mater.* **2004**, *16*, 81.

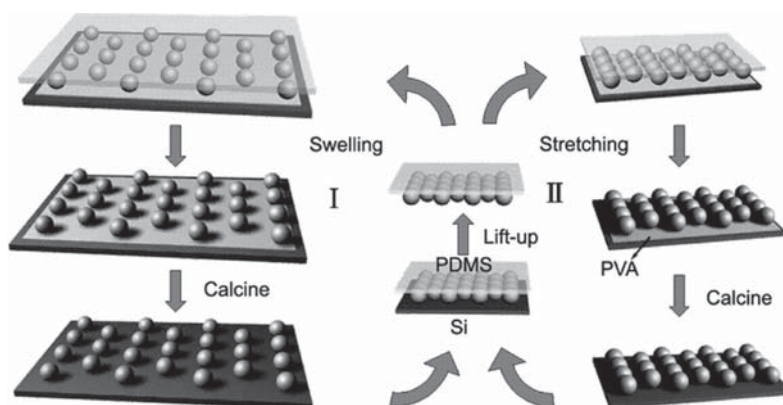


**Figure 1.** Schematic illustration of the procedure for the fabrication of 2D ncp colloidal microsphere arrays with tunable lattice spacing and structures.

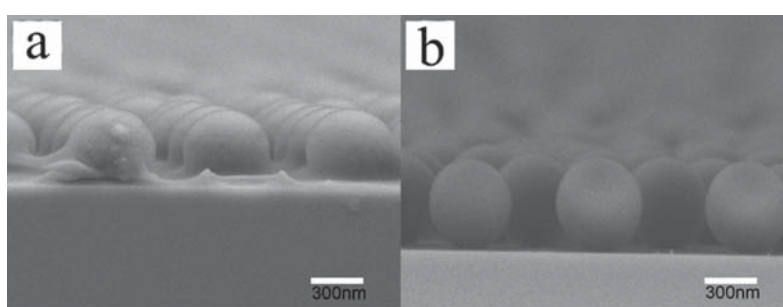


**Figure 2.** A section SEM image of the ncp arrays (a) sank into PVA film and (b) after sintering at 400 °C for 2 h.

fabrication of 2D ncp colloidal microsphere arrays. In the first stage, hcp microspheres which are in physical contact to each other are transferred onto the surface of a PDMS elastomer sheet. The PDMS sheet was then swollen with toluene (process I) or stretched along one direction (process II). Both two procedures caused expansion in the surface area of PDMS sheet. The microspheres stuck to the elastomer surface moved together with the expansion, which made them separate from each other. The obtained 2D ncp microsphere array was then transferred to a substrate coated with PVA, which had a stronger interaction with microspheres than PDMS. Because the swelling and the stretching deformation of PDMS sheet were limited within a certain range, we employed here a cycling process of the above steps after removing the PVA layer. From a cross-sectional SEM image of the ncp colloidal microsphere arrays (Figure 2a), we can see that the silica microspheres sink into the PVA film for 25 nm after the transfer printing. By employing a sintering process to remove the PVA layer, the microspheres fell on the substrate without changing the colloidal structure (Figure 2b), which enabled further cycles of lift-up and transfer printing. It was worth noting that PVA film as less than 50 nm were chosen in transfer printing process to avoid the distortion of ncp arrays during the sintering of PVA layer.

Since the solvent swelling behavior of PDMS is isotropic, the lattice spacing of colloidal crystal increase uniformly in all directions, which will not change the lattice structure. By controlling the cycling times of process I, the lattice spacing of the ncp arrays can be increased gradually to a desired value. Alternatively, with mechanical deformation of PDMS (process II), the lattice spacing will only be enlarged along the stretching direction, which will change the lattice structure. Combination of these two strategies allows for continuous changing of both the lattice

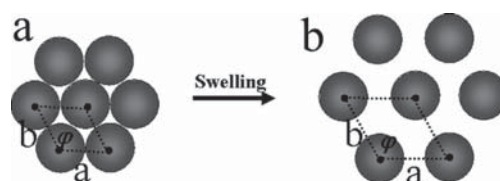


**Figure 3.** Schematic illustration of transformation of a modulated PDMS membrane with a close-packed hexagonal lattice array (a) ( $|a| = |b| = d$  and  $\varphi = 120^\circ$ ) to an optional lattice parameter via swelling deformations (b) ( $|a| = |b| = xd$  and  $\varphi = 120^\circ$ ).

spacing and the crystal lattice structure for the as-prepared 2D colloidal crystals.

**2. Control of the Lattice Spacing.** Basically, a 2D lattice is described with two translation vectors ( $a$  and  $b$ ) and the angle  $\varphi$  between them. In case of close-packed colloidal microsphere arrays in hexagonal Bravais lattice, the parameters are  $|a| = |b| = d$  (diameter) and  $\varphi = 120^\circ$  (Figure 3a). When the lattice spacing of the colloidal microsphere arrays was steadily adjusted by utilizing the solvent swelling behavior of the PDMS stamp (process I), since PDMS is expanded isotropically in all directions during the swelling process, we could get 2D ncp colloidal microsphere arrays with  $|a| = |b| = xd$  and  $\varphi = 120^\circ$  ( $x$  is an arbitrary number greater than 1, Figure 3b). Here we show that the lattice spacing could be increased by multiple lift-up and transfer printing using pure toluene as the swelling solvent during all the processes. Figure 4a shows the SEM image of an original silica colloidal microsphere array in hexagonal lattice structure. Each silica microsphere with an average diameter of  $\sim 560$  nm contacts with six neighboring microspheres. After one cycle of process I, the lattice spacing of the obtained crystal structure increased to  $(1.49 \pm 0.03)d$  (Figure 4b,  $|a| = |b| = (1.49 \pm 0.03)d$



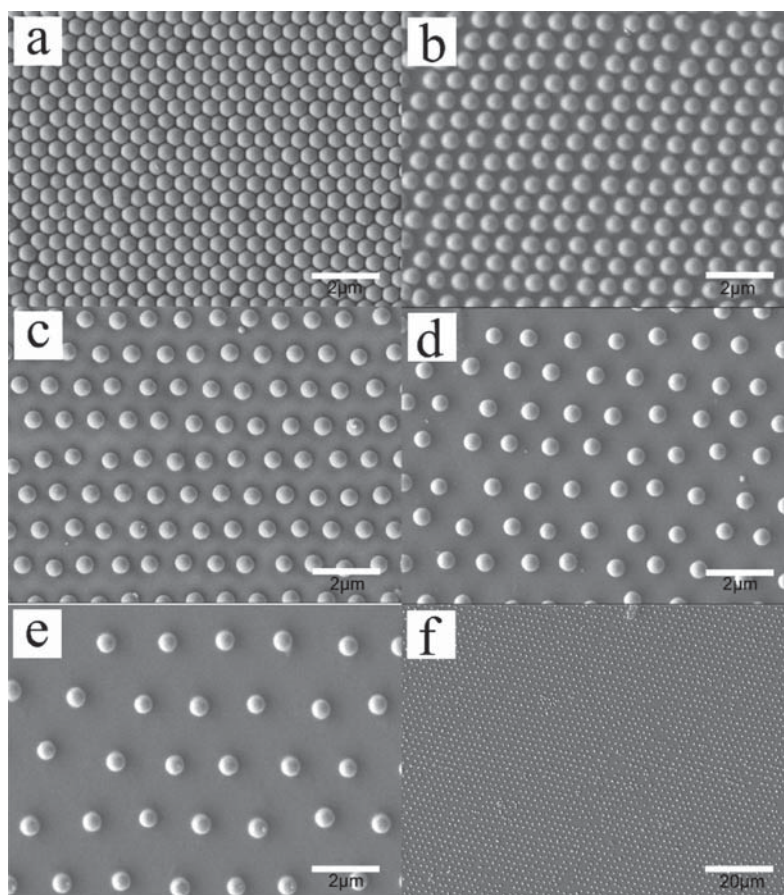


**Figure 4.** (a) SEM image of the 2D hcp arrays of 560 nm silica microspheres assembled on a silicon wafer by the evaporation of suspension ( $|a| = |b| = d$  and  $\varphi = 120^\circ$ ). (b) SEM image of the hexagonal ncp arrays on a PVA-coated substrate fabricated by swelling the PDMS film with pure toluene ( $|a| = |b| = (1.49 \pm 0.03)d$  and  $\varphi = 120^\circ$ ); SEM image of the hexagonal ncp array obtained by employing (c) two ( $|a| = |b| = (2.16 \pm 0.05)d$  and  $\varphi = 120^\circ$ ), (d) three ( $|a| = |b| = (3.18 \pm 0.08)d$  and  $\varphi = 120^\circ$ ), and (e) four ( $|a| = |b| = (4.61 \pm 0.02)d$  and  $\varphi = 120^\circ$ ) cycles of process I. (f) Low-magnification SEM image of the hexagonal ncp array in (e).

and  $\varphi = 120^\circ$ ). After the second cycle process I, the lattice spacing further increased to  $(2.16 \pm 0.05)d$  (Figure 4c,  $|a| = |b| = (2.16 \pm 0.05)d$  and  $\varphi = 120^\circ$ ), which was about 1.49 times to  $(1.49 \pm 0.03)d$ . Adding more cycles will increase the lattice spacing accordingly, e.g.,  $(3.18 \pm 0.08)d$  (Figure 4d,  $|a| = |b| = (3.18 \pm 0.08)d$  and  $\varphi = 120^\circ$ ) for the third cycle and  $(4.61 \pm 0.02)d$  for the fourth cycle (Figure 4e,  $|a| = |b| = (4.61 \pm 0.02)d$  and  $\varphi = 120^\circ$ ). Large area SEM image of Figure 4e (Figure 4f) indicates that the microspheres were homogeneously distributed with highly uniform separations, and long-range ordering (more than  $100 \mu\text{m}^2$ ) was well preserved after multiple swelling procedures.

According to the data of the first experimental cycle, we can theoretically conclude that the average swelling magnitude of PDMS elastomer with pure toluene is 1.49. Then the lattice spacing after multiple cycles could be given by  $1.49^n$ , where  $n$  represents the number of cycles repeated. This means that the ultimate distance between neighboring packed microspheres has an exponential increase to the swelling times. Our experimental results of the lattice spacing in additional cycles are consistent with this exponential relationship, which proves the controllability of our cyclical procedure.

As we reported before, the degree of swelling could be controlled by using toluene/acetone mixed solvents in different mixing ratios.<sup>35</sup> By flexibly manipulating the concentration of toluene during each swelling process, we could tune the lattice spacing of the resulting system continuously from  $1d$  to  $(4.61 \pm 0.02)d$  in four cycles and larger lattice spacing could be

realized by simply increasing the cycle number. Here we use toluene/acetone cosolvents to control the degree of swelling in each cycle. Figure 5 gives the relationship between the lattice spacing and the volume ratio of toluene and acetone in the swelling solvent for different cycles. The manipulation of multiple cycles was that the last cycle was based on the former cycles with pure toluene swelling. All results shown in these curves were reproduced several times to ensure the reliability of the method proposed herein. It was clear from the curves that the lattice spacing was a continuous regulation from  $d$  to  $(3.18 \pm 0.08)d$  even greater by increasing the cycle number. We also find in these results that the slopes of lines are increased acutely by increasing the cycle times, which means that the increased value of lattice spacing grows gradually with higher cycle times.

On the basis of the experimental results, by controlling the solution concentration of toluene and manipulating the cyclical times of process I, we can implement experimental steps to obtain any given ncp hexagonal array designed. For example, if an ncp array with  $|a| = |b| = 3.5d$  and  $\varphi = 120^\circ$  is needed (the diameter of microsphere given is 560 nm), we have information from the given conditions that the lattice spacing is 1960 nm, and then we deduce from the working curve a cycle times of 3 pure toluene swelling and a concentration of 8.2% toluene swelling via curve simulation. After these four cycles, the desired ncp arrays could be obtained. Detailed example is shown in the Supporting Information.

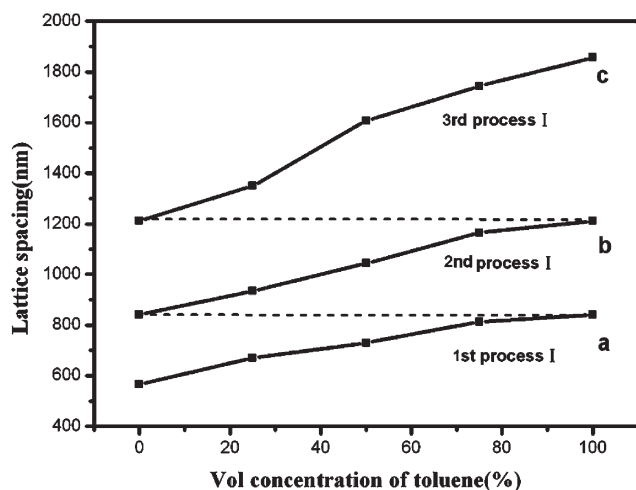


**Figure 5.** Lattice spacing (nm) versus the volume concentration of toluene in solution for ncp colloidal spheres fabricated by operating process I (a), the second process I based on one pure toluene of process I (b), and the third process I based on two cycles of process I with pure toluene (c).

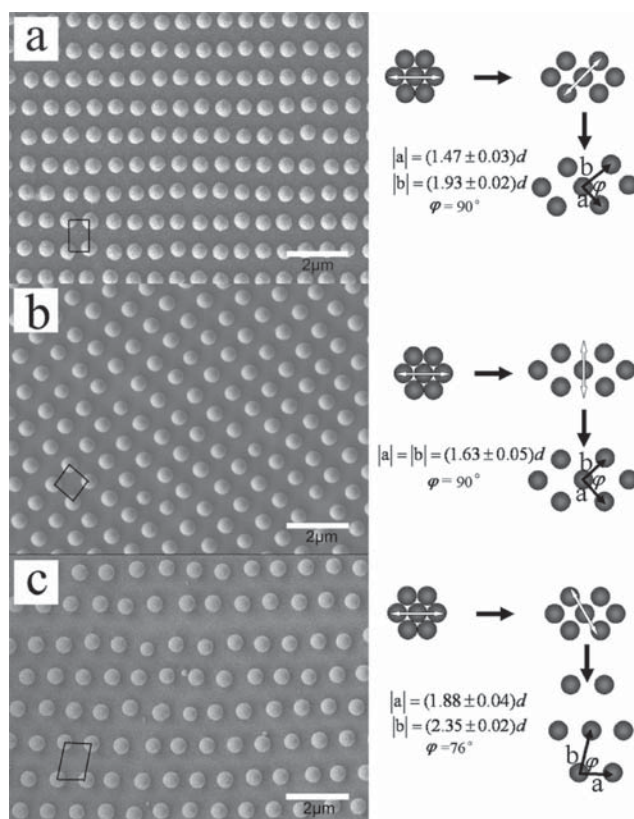


**Figure 6.** SEM images of (a) rectangular microsphere arrays, (b) square microsphere arrays, and (c) oblique microsphere arrays obtained through circular stretching process.

**3. Control of the Lattice Structures.** When we stretched the colloidal crystal-loaded PDMS sheet, the lattice structure could be changed due to the anisotropic deformation (process II). In other words, anisotropic stretching can change the symmetry of original structures, namely, the two vectors and the angle between them, which can be used to adjust the lattice structures. The magnitude of stretching is usually described with a draw ratio  $\delta$  defined as  $l/l_0$ , where  $l_0$  and  $l$  are the lengths of a sample before and

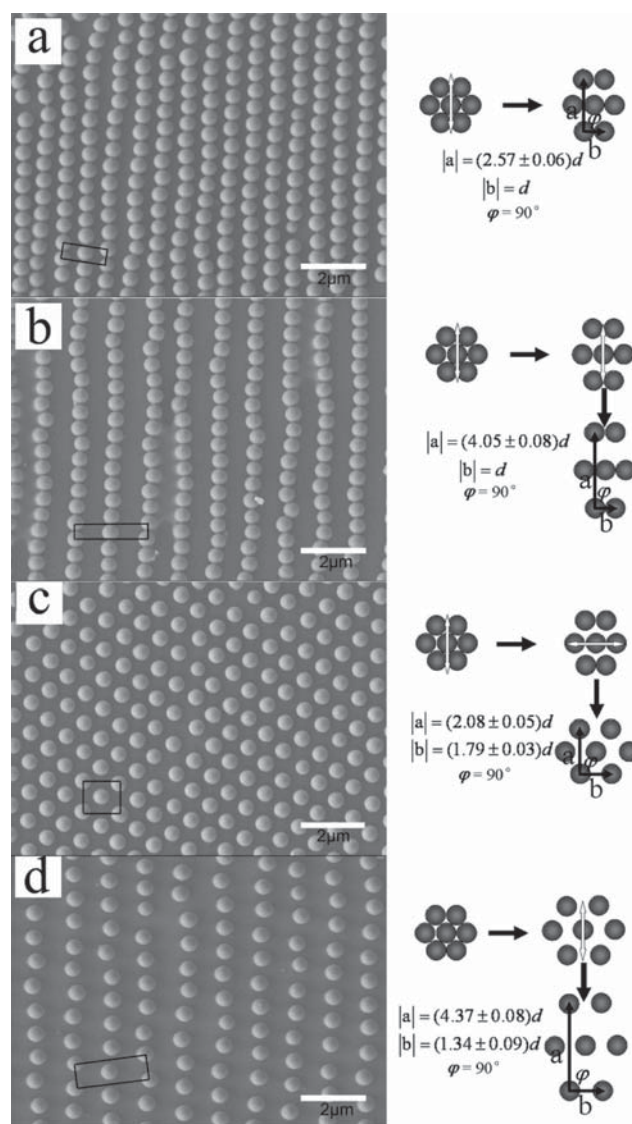


**Figure 7.** SEM images of centered rectangular arrays with different parameters fabricated by one stretching process (a); two cycles of stretching process along the same direction (b); changing the stretching directions of figure b (c) and introducing one swelling process into one stretching process (d).

after stretching. The draw ratio and direction could be controlled macroscopically by the elongation of PDMS film. Therefore, we applied the method of cycle stretching to produce other 2D Bravais lattices, and the stretching direction was described with the vectors of hexagonal Bravais lattice as reference. Here, a rectangular microsphere array (Figure 6a,  $|a| = (1.47 \pm 0.03)d$ ,  $|b| = (1.93 \pm 0.02)d$ , and  $\varphi = 90^\circ$ ) was obtained via two cycles of stretching. In the first cycle, the hcp microsphere arrays were stretched along  $a$ -axis by about 177% while maintaining the length of other directions. In the second cycle, the microspheres arrays obtained in the first cycle were transferred to another PDMS sheet, which was then stretched along the direction with an angle of  $45^\circ$  to  $a$ -axis by about 137%. Figure 6b shows a SEM image of square lattice structure ( $|a| = |b| = (1.63 \pm 0.05)d$  and  $\varphi = 90^\circ$ ) fabricated by stretching the PDMS film along  $a$ -axis by about 258% in the first cycle and along the direction perpendicular to  $a$ -axis by about 149% in the second cycle. An oblique lattice structure ( $|a| = (1.88 \pm 0.04)d$ ,  $|b| = (2.35 \pm 0.02)d$ , and  $\varphi = 76^\circ$ ) was obtained (Figure 6c) by a two-cycle stretching.



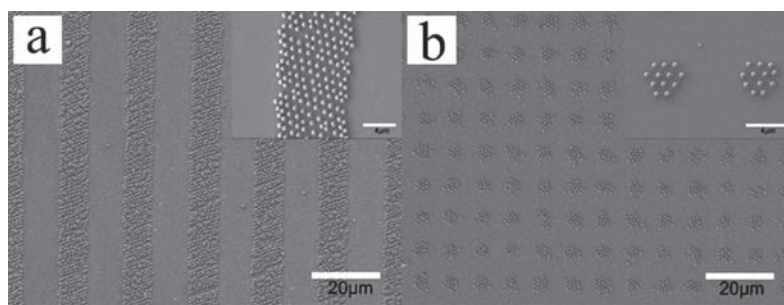


**Figure 8.** SEM images of (a) parallel lines and (b) cylinders of the 2D ncp sphere arrays on a PVA-coated substrate.

The whole process was that the first draw along  $a$ -axis by about 188% and the second draw extending to  $b$ -axis by about 263%.

Controlling both the direction and the strain can be applied to particular Bravais lattices, which can also be applied to regulate the lattice parameters of the same lattice structure. For example, a centered rectangular lattice structure ( $|a| = (2.57 \pm 0.06)d$ ,  $|b| = d$ , and  $\varphi = 90^\circ$ ) can be obtained by stretching the PDMS stamp along the direction perpendicular to  $a$ -axis by about  $\delta = 157\%$  (Figure 7a). When a repeated stretching along the same direction by about 153% without changing the length of other direction, the same lattice structure but different lattice parameters with  $|a| = (4.05 \pm 0.08)d$ ,  $|b| = d$ , and  $\varphi = 90^\circ$  is shown in Figure 7b. Changing the stretching direction that the first draw along the direction perpendicular to  $a$ -axis by about 120% and the second draw along  $a$ -axis by about 171%, centered rectangular arrays with  $|a| = (2.08 \pm 0.05)d$ ,  $|b| = (1.79 \pm 0.03)d$ , and  $\varphi = 90^\circ$  were obtained (Figure 7c).

Furthermore, process I and process II introduce anisotropic and isotropic characteristics into the deformation process, respectively. Combination of these two processes, 2D lattice structures with more complex parameters could be fabricated. A sample is shown in Figure 7d. 2D ncp hexagonal microsphere arrays which were fabricated by swelling the PDMS with pure toluene (as indicated in Figure 4b) were stretched along the direction perpendicular to  $a$ -axis by about 178%, centered rectangular arrays with  $|a| = (4.37 \pm 0.08)d$ ,  $|b| = (1.34 \pm 0.09)d$ , and  $\varphi = 90^\circ$  were obtained.

In general, process I can be employed to achieve any desired hexagonal array structure and process II can be used to fabricate other four 2D Bravais lattice structures with enriching the lattice parameters by changing the direction and the draw strain. Combining these two procedures, not only the lattice spacing but also the lattice structure can be controlled, which will greatly enrich the complexity of 2D ncp colloidal crystals through rational design.

**4. Patterned Ncp Arrays of Colloidal Crystal from Lift-up Soft Lithography.** Employing PDMS stamp with micrometer-sized pattern features, we could get patterned ncp arrays. When we conducted the lift-up process with patterned PDMS stamp, ncp microspheres were lifted up to the patterned PDMS selectively. With the help of PVA, patterned ncp colloidal microsphere arrays could be transferred to the substrate. Figure 8a shows a SEM image of parallel lines consisting of 2D ncp arrays which were transferred onto a silicon substrate. These lines were  $\sim 9 \mu\text{m}$  wide and separated by  $11 \mu\text{m}$ , which agree well with the patterned feature of PDMS stamp we used. Another PDMS stamp with cylindrical pillar ultimately produced patterned hierarchical arrays of silica microspheres as indicated from Figure 8b. Both the lattice structure and the patterned crystal arrays show long-range ordering here. From the SEM image, we can also find that the average lattice spacing of the ncp arrays is

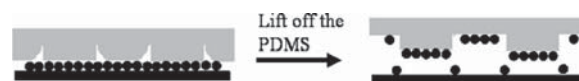


**Figure 9.** Schematic illustration of the procedure used to generate the 1D microsphere arrays using the deformable lift-up soft lithography.

about  $2.16d$ , while the pattern features of these arrays are the same as the PDMS stamp. High-magnification SEM images further prove the dual scale-ordered microstructures in the patterned arrays (see the insets in Figure 8a,b).

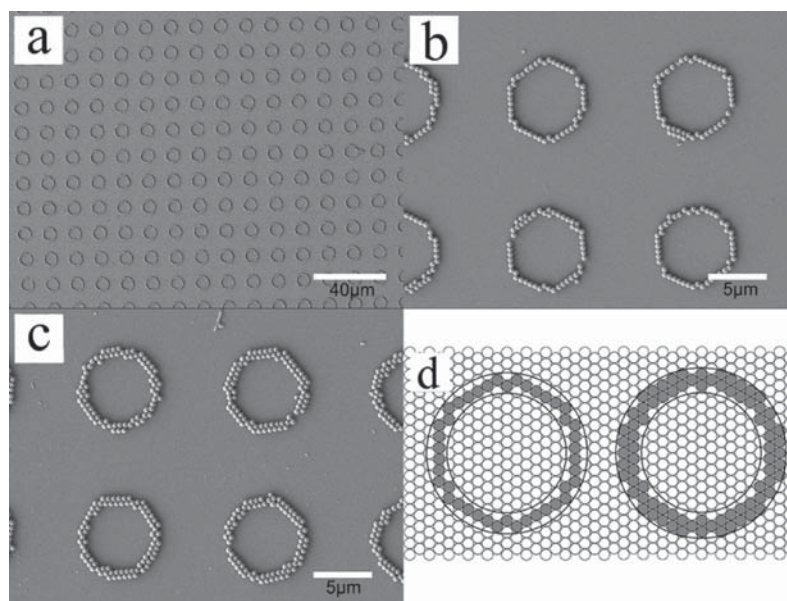
Besides the 2D deformation behavior of PDMS, patterned PDMS stamp can be deformed vertically under capillary force and mechanical stress during the transfer process.<sup>39</sup> As schemed in Figure 9, at the equilibrium state, small voids are formed around the edges of the protruding regions of the stamp. After the lift-up operation, microspheres in these areas remain and generate patterned one-dimensional (1D) ncp arrays. According to previous reports,<sup>40</sup> the deformation of PDMS can be adjusted by several factors, such as the aspect ratio, the external force, the elastic module, etc. In our work, we adjust the deformation by changing the elastic module. The mixing ratio between the polymer precursor and the curing agent directly relates to the elastic module of PDMS elastomer; thus, we simply fix all other conditions and tune this ratio for a model demonstration of our strategy.

Figure 10a shows a large area 1D ringlike microsphere array with one-microsphere width obtained using a soft PDMS stamp. The high-magnification SEM image (Figure 10b) clearly depicts that each hexagon consists of six straight 1D microsphere lines and six microspheres located in the inner vertices. The mechanism for generating the 1D microsphere hexagonal line structure was schematically illustrated in Figure 10d. The 2D hexagonal close-packed colloidal crystal film is represented by the ordered circle array, and the dark circles are the microspheres entirely located within the void region, which is further highlighted by the enclosed circles. The dark circle hexagon on the left exactly matches the microsphere structure in Figure 10b. When we increase the mixing ratio, hard elastomer allows generation of larger voids therefore gave rise to the formation of a ringlike array with double-microsphere width (Figure 10c). The same mechanism with the single-microsphere width arrays could be applied to explain this process, which was schematically illustrated in the right part of Figure 10d.

Besides the PDMS with isotropic post structures, we also tried PDMS stamp with an anisotropic strip pattern to generate 1D microsphere line array. Figure 11a shows a SEM micrograph of a

(39) Perl, A.; Reinhoudt, D. N.; Huskens, J. *Adv. Mater.* **2009**, *21*, 2257.

(40) Delamarche, E.; Schmid, H.; Michel, B.; Biebuyck, H. *Adv. Mater.* **1997**, *9*, 741.



**Figure 10.** SEM images of 1D microsphere hexagon array with one-microsphere width: (a) in large area, (b) a magnified view; (c) a high-resolution image of hexagon array with double-microsphere width; (d) a schematic illustration of the mechanism.

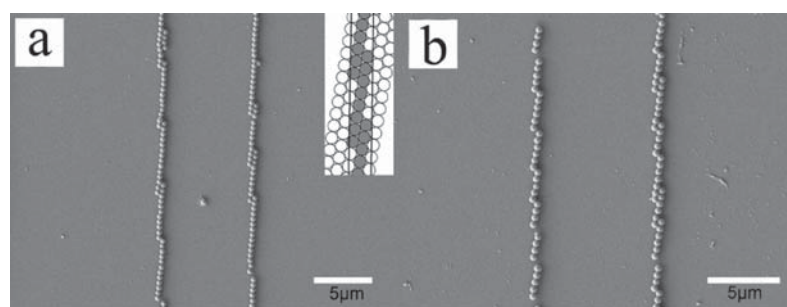


**Figure 11.** SEM images of microsphere line structures formed by utilizing (a)  $3.4^\circ$  and (b)  $9.7^\circ$  difference between the line direction and the crystalline orientation. A schematic illustration of the mechanism for generating the microsphere line structure was inserted in (a).

1D microsphere line array with one-microsphere width obtained by using a soft PDMS stamp. The line-shaped void spaces formed by the deformable PDMS had a  $3.4^\circ$  angle difference with the orientation of the colloidal crystal. We schematically illustrate the mechanism for generating the line structures in the inset of Figure 11a. The dark circle zigzag structure in the void space exactly matches the microsphere structure in Figure 11a. By adjusting the orientation differences between the line-shaped void space and the 2D colloidal crystal, we could flexibly design various 1D microsphere structures. For example, Figure 11b shows a 1D microsphere line array with different zigzag structures formed by utilizing a  $9.7^\circ$  angle mismatch between the line direction on the PDMS and the crystalline orientation of the colloidal crystal.

### Conclusion

In summary, we developed a simple and versatile method to manipulate the lattice structure and the lattice spacing of 2D ncp colloidal crystal arrays in a controlled fashion based on PDMS-assisted deformation strategy. This method exploits the self-assembly of colloidal crystal arrays followed by lift-up lithogra-

phy that transfers large areas of 2D hcp microsphere arrays onto PDMS stamp. Taking advantage of isotropic solvent swelling and anisotropic mechanical stretching of PDMS stamp, the lattice feature could be changed step by step. Combining circular lift-up process and modified soft lithography technique, 2D ncp colloidal crystal with Bravais lattice structures and controllable lattice features could be obtained as well as new types of patterned colloidal crystals. These novel structures could be used as molds in colloidal crystal for patterning other materials such as porous inorganic films and nanowires. They can also act as prototype models in theory simulation fields for optical materials.

**Acknowledgment.** This work was supported by the National Natural Science Foundation of China (Grants 20534040 and 20874039) and the National Basic Research Program of China (2007CB936402).

**Supporting Information Available:** An example of designing experimental steps to achieve a given goal via curve simulation and theoretical calculation. This material is available free of charge via the Internet at <http://pubs.acs.org>.